Structure-guided Deep Multi-View Clustering

Jinrong Cui, Xiaohuang Wu, Haitao Zhang, Chongjie Dong, and Jie Wen*, *Senior Member, IEEE*

***Abstract*—Deep multi-view clustering seeks to utilize the abundant information from multiple views to improve clustering performance. However, most of the existing clustering methods often neglect to fully mine multi-view structural information and fail to explore the distribution of multi-view data, limiting clustering performance. To address these limitations, we propose a structure-guided deep multi-view clustering model. Specifically, we introduce a positive sample selection strategy based on neighborhood relationships, coupled with a corresponding loss function. This strategy constructs multi-view nearest neighbor graphs to dynamically redefine positive sample pairs, enabling the mining of local structural information within multi-view data and enhancing the reliability of positive sample selection. Additionally, we introduce a Gaussian distribution model to uncover latent structural information and introduce a loss function to reduce discrepancies between view embeddings. These two strategies explore multi-view structural information and data distribution from different perspectives, enhancing consistency across views and increasing intra-cluster compactness. Experimental evaluations demonstrate the efficacy of our method, showing significant improvements in clustering performance on multiple benchmark datasets compared to state-of-the-art multi-view clustering approaches.**

***Index Terms*—Multi-view clustering, deep learning, contrastive learning, representation alignment.**

I. INTRODUCTION

Clustering is a crucial aspect of unsupervised learning in machine learning, focusing on grouping intrinsically related samples into clusters without the need for label information. Clustering techniques have shown great potential across various domains, including image segmentation [1], [2], cross-modal hashing [3], [4], [5], and data mining [6], [7], [8], [9]. With the increasing richness and diversity of data sources, data described from multiple perspectives, known as multi-view data, has become more prevalent. Multi-view clustering (MVC) has risen to prominence in research.

Traditional MVC methods mainly include subspace-based methods [10], [11], [12], graph-based methods [13] [14], [15], [16], and matrix factorization-based methods [17], [18], [19]. Subspace-based methods aim to capture low-dimensional embedding subspaces from the high-dimensional feature spaces of each view and subsequently learn a unified subspace representation. Graph-based methods mine the inherent relationships in data by constructing graph structures and applying graph partitioning algorithms to achieve optimal clustering results. Matrix factorization-based methods leverage matrix decomposition techniques to handle multi-source data, revealing the underlying structure of the data. However, traditional MVC methods are limited in their feature extraction capabilities and are sensitive to noise, which restricts their clustering performance to some extent.

As we all know, deep neural networks have powerful nonlinear mapping capabilities in feature representation learning. This capability has significantly propelled the development of deep MVC methods [20], [21], [22], [23], [24], [25] and garnered widespread attention from researchers. Deep MVC methods effectively learn representations for each view by constructing encoder networks, capturing complex patterns in multi-view data. Additionally, these methods design loss functions at various granularities, such as instance-level and view-level, to further explore the deep semantic information within data, significantly improving clustering performance. With these advantages, a series of deep learning-based clustering methods have achieved impressive performance on multi-view datasets, demonstrating great potential for complex clustering tasks.

Despite the introduction of numerous MVC methods, especially deep learning-based clustering approaches in recent years, they still face several challenges that limit their performance. 1) Many existing contrastive-based deep MVC methods overlook local structural information within views. These methods typically treat the same instance across different views as a positive pair and all other instances as negative pairs. While this approach ensures the accuracy of positive pairs, it neglects the reliability of negative pairs. Among the selected negative pairs, false negatives with high correlation to positive samples may arise, resulting in the loss of structural information and hindering the learning of discriminative features, which negatively impacts clustering performance. 2) Some existing methods aim to align representations across views but fail to leverage both shared and latent information from each view effectively. Strict alignment can lead to the loss of valuable latent structural information in the cross-view embedding space, limiting the model's ability to fully exploit the rich information of multi-view data.

To address the aforementioned issues, we design a Structure-Guided deep Multi-View Clustering framework (SGMVC), as illustrated in Fig. 1. The proposed framework primarily consists of three modules: the multi-view encoder-decoder module, the local structure learning module, and the embedding structure learning module. Specifically, the multi-view encoder-decoder module is utilized to learn latent

Jinrong Cui is with the College of Mathematics and Informatics, South China Agricultural University, Guangzhou, 510620, China (Email: tweety1028@163.com).

Xiaohuang Wu is with the College of Mathematics and Informatics, South China Agricultural University, Guangzhou, 510620, China (Email: wuwuxxxh@163.com).

Haitao Zhang is with the Shenzhen Institute for Advanced Study, University of Electronic Science and Technology of China, Shenzhen 518110, China; (Email: zhanght23 @uestc.edu.cn).

Chongjie Dong is with the Dongguan Polytechnic, Dongguan, China; (Email: 280292167@qq.com).

Jie Wen is with the Shenzhen Key Laboratory of Visual Object Detection and Recognition, Harbin Institute of Technology, Shenzhen 518055, China (Email: jiewen_pr@126.com).

Corresponding author: Jie Wen.

representations from each view. The local structure learning module enhances the extraction of local structural information by introducing a refined cross-view consistent neighbor selection strategy, effectively increasing reliable positive sample pairs, which promotes the learning of discriminative information for samples, thereby benefiting the clustering task. Meanwhile, to further explore the structural information within the data, the embedded structure learning module introduces Gaussian distributions to uncover structural information in the embedded space, optimizing embedding differences to achieve more consistent structural alignment, thus improving clustering performance. The following are this paper's primary contributions:

- We propose a deep multi-view clustering model that effectively uncovers both the local structural information and the latent structural information of the data through multi-view neighborhood construction and Gaussian modeling.
- A cross-view consistency-based neighbor selection strategy, combined with a neighborhood consistency-guided contrastive loss, is designed to capture structural information within views.
- Extensive experiments are conducted on five multi-view datasets, and the results validate the effectiveness of the proposed SGMVC.

II. RELATED WORK

In this section, we review the related work on multi-view clustering and contrastive learning, providing a brief introduction to them below.

A. Traditional Multi-view Clustering

Traditional multi-view clustering methods are commonly divided into multi-view graph clustering and multi-view subspace clustering. Specifically, multi-view graph clustering learns distinct graph structures for each view and integrates them through regularization strategies to produce the final clustering results. For example, [26] automatically assigns weights to each view, learns individual graphs for each view, and generates clustering results directly on the fused graph. [27] employs graph filtering techniques to smooth node representations, learns a consensus graph that represents the overall data structure, and flexibly explores higher-order node relationships. In addition, [28] generates latent segmentation representations based on anchor graphs and introduces a label discretization mechanism to directly obtain a binary clustering indicator matrix. Multi-view subspace clustering focuses on learning a unified subspace representation from the specific subspaces of each view. For instance, [29]proposes a new self-representation property that combines consistency and specificity to capture the intrinsic relationships of multi-view data. [30] incorporates an angle-based regularizer to effectively leverage the correlation consensus among multi-view data. However, these traditional methods face limitations in handling complex data, as they struggle to capture deep semantic information, which restricts their performance in more complex multi-view scenarios.

B. Deep Multi-view Clustering

Driven by the rapid advancements in deep learning for unsupervised learning, deep networks have exhibited exceptional capabilities in extracting features and learning representations. Consequently, deep MVC methods leveraging deep representation learning have garnered significant attention. Autoencoders are extensively applied in multi-view scenarios. For example, [31] proposes a selective alignment mechanism to preserve the model's capability to prioritize different views and avoid losing critical information during alignment. Similarly, [32] introduces a method that automatically selects features to extract complementary information from views while filtering out irrelevant noise. This method sustains strong clustering performance even with an increasing number of views, mitigating performance degradation risks due to view redundancy. Additionally, deep representation-based MVC methods integrate graph neural networks GNNs to exploit both the structural and attribute information of views via GCN encoders. [33] employs dual encoders to reconstruct high-dimensional features and integrate low-dimensional consensus information, achieving an optimal multi-view attributed graph representation. Similarly, [34] uses GCN encoders to learn a self-expression coefficient matrix and applies block-diagonal representation constraints to derive coefficients that effectively capture the underlying clustering structure. [35] adopts a late fusion alignment strategy by evaluating the importance of instances across different views and applying weighted processing. Additionally, it introduces a regularization term to enhance the efficiency of information integration.

C. Contrastive Learning

In recent years, contrastive learning, as a popular self-supervised representation learning method, has attracted great attention from researchers. For every sample in the feature space, the basic idea is to create positive and negative sample pairs with the goal of pushing negative pairs apart and bringing positive pairs closer together. In the realm of unsupervised learning, this concept has been broadly adopted and has produced remarkable results. For instance, MOCO [36] introduces a momentum update mechanism to align the representations of positive and negative pairs, effectively enhancing the performance of unsupervised representation learning. Another study, SimCLR [37], further enhances representation learning by maximizing the similarity between different augmented views of the same data sample.

The achievements of contrastive learning have greatly contributed to the progress of deep clustering. For example, [38] integrates the concepts of feature alignment and reconstruction, designing an enhanced feature-level contrastive learning module as well as an enhanced cluster-level contrastive learning mechanism. [39] proposes a specialized contrastive loss function that employs pseudo-labels to analyze the consistency between different modalities in cross-modal data. By integrating clustering layers, this approach can directly predict the clustering labels of samples while also handling unseen new samples. [40] addresses incomplete multi-view data using multi-level imputation and multi-level contrastive alignment.

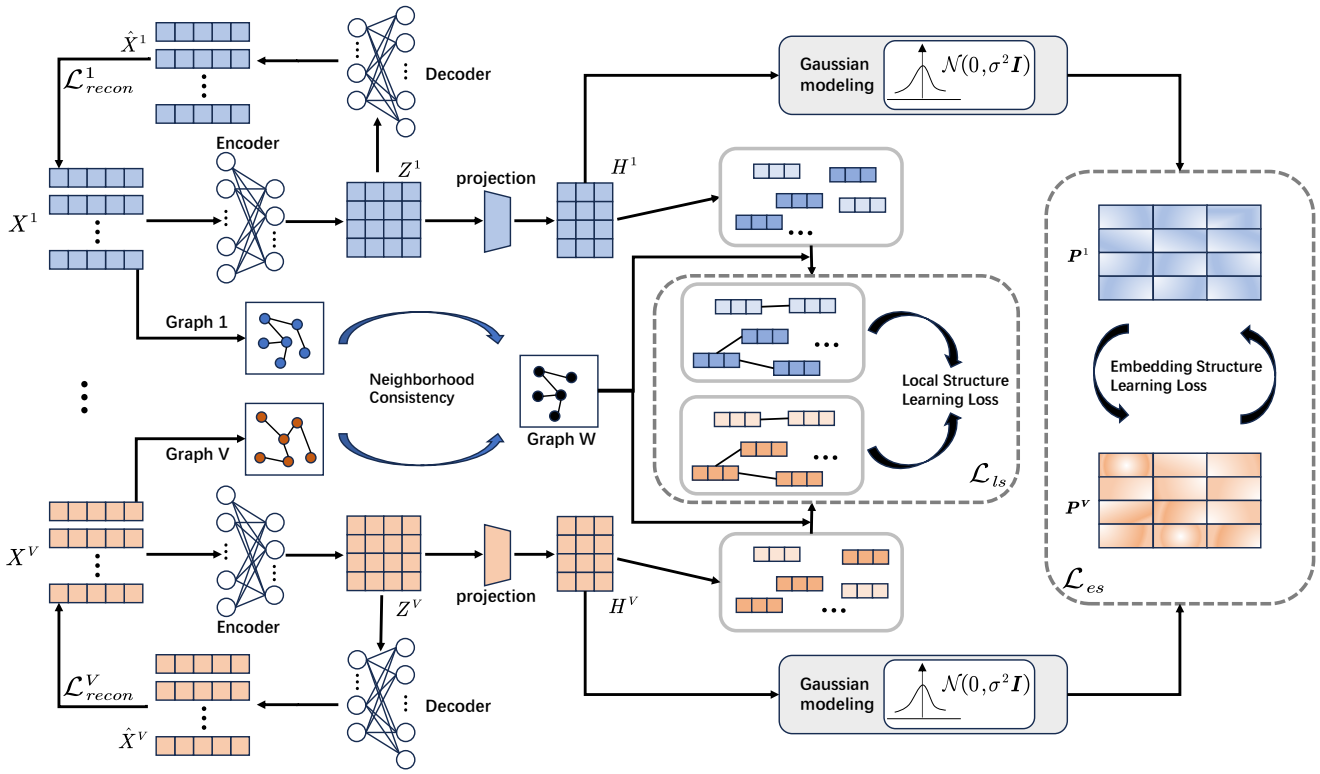

Fig. 1: The framework of SGMVC. The framework includes: Multi-view Encoder-Decoder Module, which learns feature representations through view-specific encoder-decoder structures. Local Structure Learning Module, reducing false negative samples based on sample neighborhood relationships to enhance instance discriminability. Embedding Structure Learning Module, uncovering latent structural information using Gaussian sampling to minimize embedding discrepancies of the same instance across different views.

TABLE I: Notations and their descriptions.

Notation	Description
$\mathbf{X}$	The multi-view dataset
X^v	Data input for view v
V	Number of views
N	Number of samples
C	Number of clusters
x_i^v	Vector feature of the i-th sample in the v-th view
z_i^v	Latent representation of the i-th sample of the v-th view
$\hat{x}_i^v$	Reconstruction feature of the i-th sample in the v-th view
h_i^v	Embedding representation of the i-th sample of the v-th view
$s\left(h_p, h_q\right)$	Cosine similarity of sample p and sample q
$W_{i,j}^{v,w}$	The indicator matrix represents whether the two samples are neighbors
p_i^v	The i-th sample of the v-th view based on Gaussian sampling
λ_1, λ_2	Balance parameters within the objective loss function

III. Methodology

Task Statement: Given a multi-view dataset $\mathbf{X} = \{X^v \in \mathbb{R}^{N \times d_v}\}_{v=1}^{V}$ consisting of V views and N samples, where d_v is the dimension of the v-th view. The goal of multi-view clustering is to assign the N samples into C distinct clusters.

Table I summarizes the variables used in our model and their details. In this section, we will detail the three modules of our model as shown in Fig. 1.

A. Multi-view Encoder-Decoder Module

In MVC tasks, the original multi-view data often contains critical view-specific discriminative information, consensus representations shared across views, and other redundant noise. Leveraging the strong feature extraction capabilities of autoencoders in unsupervised models, we introduce a specific autoencoder for each view to extract latent information from the corresponding view. Specifically, f^v refers to the encoder, and g^v refers to the decoder corresponding to the v-th view. Given the encoder for the v-th view, the latent information of the i-th sample is represented as:

$$z_i^v = f^v\left(x_i^v; \varphi^v\right), \tag{1}$$

where $z_i^v \in \mathbb{R}^d$ represents the extracted latent representation, d denotes the dimension of the latent representation, and φ^v represents the parameters of the encoder for the v-th view. By reconstructing x_i^v through the decoder, the obtained reconstructed samples can be represented as:

$$\hat{x}_i^v = g^v\left(z_i^v; \psi^v\right) = g^v\left(f^v\left(x_i^v; \varphi^v\right); \psi^v\right), \tag{2}$$

where $\hat{x}_i^v$ indicates the reconstruction of the i-th sample within the v-th view, with ψ^v denoting the parameters of the corresponding decoder.

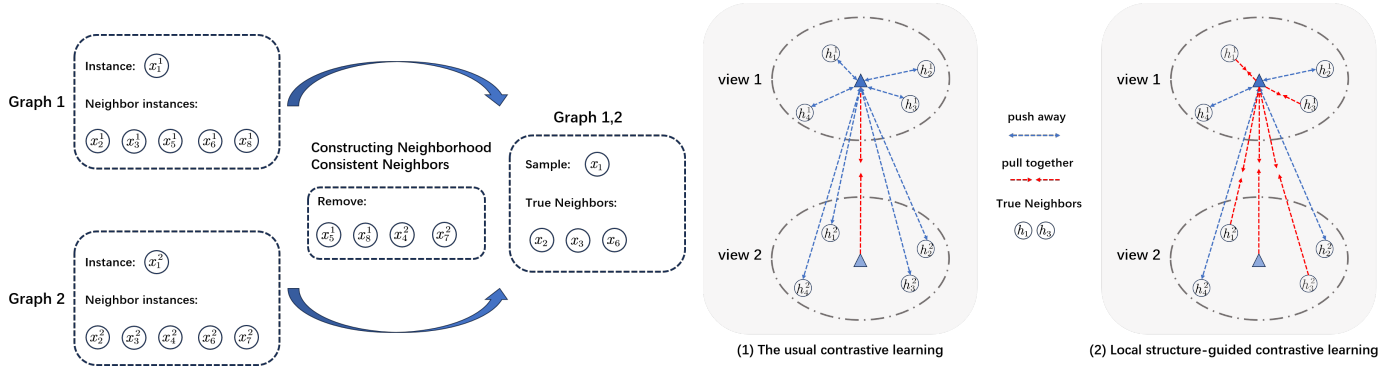

(a) Constructing neighborhood consistency neighbors. (b) Constructing positive and negative sample pairs.

Fig. 2: (a) Constructing neighborhood consistency neighbors: An instance is considered a true neighbor only if it is consistently identified as a neighbor in both views. (b) Contrastive learning: (1) General contrastive learning typically considers only the same instance across different views as positive samples. (2) By incorporating neighbors, it enables better learning of discriminative features and enhances intra-cluster compactness.

To train the autoencoders for all views, the reconstruction loss can be formulated as:

$$\mathcal{L}_{recon} = \sum_{v=1}^{V} \mathcal{L}_{recon}^{v} = \sum_{v=1}^{V} \sum_{i=1}^{N} \|x_i^v - \hat{x}_i^v\|_2^2. \tag{3}$$

B. Local Structure Learning Module

In multi-view scenarios, to explore the consistency and complexity relationships between different views, Contrastive Learning (CL) can be employed to align the feature distributions of n views. In contrastive learning, different view representations of the same sample are typically constructed as a positive sample pair, while the other two instances from different samples are formed into negative sample pairs. The learning process aims to maximize the similarity within positive pairs and minimize it between negative pairs, ensuring the capture of both consistency and discriminative characteristics in multi-view data. Similar to SimCLR, we use the instance-level feature projection head to project the potential representation Z^v of the v-th view into the lower-dimensional embedding space H^v, which promotes efficient contrast learning. Within the new feature embedding space, cosine similarity is used to measure the similarity between two samples.

$$s\left(h_i^v, h_j^u\right) = \frac{\left(h_i^v\right)^T h_j^u}{\|h_i^v\| \|h_j^u\|}. \tag{4}$$

An essential part of contrastive learning involves building positive and negative pairs. However, the previous strategy oversimplifies the construction of these pairs, failing to fully leverage the structural information from the views and to incorporate potential positive sample pairs. This limitation can undermine the consistency and discriminative power between samples, thereby negatively impacting clustering performance. Intuitively, within the original feature space, samples belonging to the same class ought to be located in close proximity to one another. Based on this observation, we construct a nearest neighbor graph in the original feature space and use the neighbor relationships to build additional reliable positive pairs, addressing the previously mentioned issue. Regarding the v-th view, the formulation for constructing the nearest neighbor graph is as follows:

$$w_{i,j}^v = \begin{cases} 1 & \left(x_i^v \epsilon \Lambda\left(x_j^v\right)\right) \ or \ \left(x_j^v \epsilon \Lambda\left(x_i^v\right)\right) \\ 0 & otherwise \end{cases}, \tag{5}$$

where $\Lambda\left(x_i^v\right)$ represents the set of instances closest to x_i^v in the v-th view.

However, in MVC scenarios, different views usually have distinct nearest-neighbor graphs because their original feature spaces tend to exhibit variations. To address this issue, we introduce a refined neighbor selection criterion to ensure consistency across views. As shown in Fig. 2a, in our method, for any pair of views, an instance is considered as a true neighbor only if it is consistently identified as a neighbor in at least two views. In other words, we can construct several refined neighbor graphs as follows:

$$W_{i,j}^{vu} = \begin{cases} 1 & \left(w_{i,j}^v = 1\right) \ and \ \left(w_{i,j}^u = 1\right) \\ 0 & otherwise \end{cases}, \tag{6}$$

where $W_{i,j}^{vu}$ and $W_{i,j}^{uv}$ are identical.

This reduces the introduction of incorrect positive pairs caused by noise. By maintaining consistency in neighbor selection across multiple views, we can construct a reliable set of positive sample pairs $\mathcal{P}_i^{vu}$ as follows:

$$\mathcal{P}_i^{vu} = \{j \mid W_{i,j}^{vu} = 1, \ \forall j \in [1, N]\}. \tag{7}$$

Building on the positive and negative sample pair construction as described in Fig. 2b, we compute inter-view contrastive loss within the new feature embedding space. The contrastive loss function between views is defined as follows:

$$\mathcal{L}^{vu} = -\frac{1}{N} \sum_{i=1}^{N} \log \frac{\sum_{j \in \mathcal{P}_i^{vu}} e^{s\left(h_i^v, h_j^u\right)/\tau}}{\sum_{j=1}^{N} e^{s\left(h_i^v, h_j^u\right)/\tau} - e^{1/\tau}}, \tag{8}$$

where τ denotes the temperature parameter.

The total contrastive learning loss function can be formulated as:

$$\mathcal{L}_{ls} = \frac{1}{2}\sum_{v=1}^{V}\sum_{u\neq v}\mathcal{L}^{vu}. \tag{9}$$

C. Embedding Structure Learning Module

The heterogeneity and diversity of data sources lead to significant differences in the feature spaces of different views. This heterogeneity among views affects clustering performance and complicates view alignment, particularly when learning a shared embedding representation. We aim to effectively capture shared information across views during the embedding learning process while preserving potential structural information within the embedding space. In the Gaussian distribution modeling space, there is an inherent correlation between the center point and its surrounding samples [41]. With this objective in mind, we introduce a probabilistic modeling approach utilizing Gaussian distributions to uncover hidden structural information.

Specifically, for the samples in each view, we introduce a Gaussian distribution to model their feature representations. We assume that the feature representations of the samples follow the following distribution:

$$p_i^v \sim \mathcal{N}\left(h_i^v, \eta^2 \boldsymbol{I}\right), \tag{10}$$

where η is the parameter that controls the variance of the sampling, $\boldsymbol{I}$ is the identity matrix, and p_i^v is the sample obtained by sampling. Based on this distribution, we perform Gaussian sampling on the sample representation:

$$p_i^v = h_i^v + \eta\epsilon, \tag{11}$$

where ϵ is random noise sampled from a standard Gaussian distribution.

The generated sample p_i^v can be considered as a positive example within the same class as the original sample h_i^v through this method. To further leverage the latent structural information across views, we introduce the following loss function:

$$\mathcal{L}_{es} = \sum_{v=1}^{V}\sum_{u\neq v}\sum_{i=1}^{N}\|l\left(p_i^v\right) - l\left(p_i^u\right)\|_2^2, \tag{12}$$

where $l\left(\cdot\right)$ denotes the prediction network [42]. By introducing this probabilistic framework, the loss function aims to minimize the feature embedding discrepancies between the sampled results of the same sample across different views. This not only helps to uncover latent information but also ensures effective alignment of the features for the same sample across views.

D. Overall objective function

The objective function of the proposed framework primarily consists of three parts:

$$\mathcal{L} = \mathcal{L}_{recon} + \lambda_1\mathcal{L}_{ls} + \lambda_2\mathcal{L}_{es}, \tag{13}$$

where λ_1 and λ_2 are the balancing parameters for the three components of the loss. The training process of the network framework is described in Algorithm 1.

To obtain a unified clustering outcome, we perform an average-weighted combination of the representations from all views to derive a final, comprehensive representation. Using this unified representation as input, k-means clustering is applied to generate the final clustering results.

Algorithm 1: Training process of SGMVC

Input: Multi-view dataset $\mathbf{X}$, number of samples N, the cluster number C, training epoch T, and trade-off hyper-parameters λ_1, λ_2
Output: The clustering result
Initialize $\{\varphi^v, \psi^v\}_{v=1}^V$ by minimizing Eq. (3);
Construct the nearest-neighbor graph for each view by Eq. (5) and cross-view consistency neighbor graph by Eq. (6);
for *epoch = 1 to T* **do**
  compute $\mathcal{L}_{ls}$ through Eq. (9);
  Gaussian sampling is performed on each sample by Eq. (11), and then the sampled features are processed by the prediction network;
  compute $\mathcal{L}_{es}$ through Eq. (12);
  compute overall loss $\mathcal{L}$ by Eq. (13);
  network parameters are optimized by minimizing $\mathcal{L}$ through the use of the Adam optimizer;
end

IV. EXPERIMENTS

A. Datasets

Our evaluation of the proposed model is conducted across five datasets of diverse sizes, including Caltech-5V, Wiki, Reuters, Hdigit, and ALOI. Table II shows the details of these datasets.

- Caltech-5V [43]: Caltech-5V is a multi-view RGB image dataset containing 1400 samples, including feature representations extracted by five well-known conventional feature descriptors: WM, CENTRIST, LBP, GIST, and HOG.
- Wiki [44]: Wiki is a commonly used cross-modal dataset that includes 2,866 image-text pairs, covering 10 different semantic categories.
- Reuters [45]: This is a collection of textual data that includes English versions and their translations into four different languages. We make use of a subset of the Reuters dataset that contains 9,379 samples, distributed over six categories.
- Hdigit [46]: Derived from the MNIST and USPS handwritten digit datasets, Hdigit comprises 10,000 samples represented through two distinct views.
- ALOI [47]: This dataset is a subset of ALOI-1k, where four view representations are obtained by extracting color similarity, Haralick, HSV, and RGB features from each image.

B. Compared Methods and Evaluation Metric

To evaluate SGMVC, we contrast it with several traditional and deep multi-view clustering methods outlined below.

TABLE II: Description of benchmark datasets.

Dataset	Samples	Views	Clusters
Caltech-5V	1400	5	7
Wiki	2866	2	10
Reuters	9379	5	6
Hdigit	10000	2	10
ALOI	10800	4	100

- LMVSC: Large-scale Multi-View Subspace Clustering (LMVSC) [48] uses anchor graphs to build compact representations for each view and establishes a method for integrating these graphs.
- SMVSC: Scalable Multi-View Subspace Clustering (SMVSC) [49] utilizes a unified anchor graph to adaptively gather complementary information across views and concurrently assess the significance of each view.
- OPMC: One-Pass Multi-view Clustering (OPMC) [50] removes the non-negativity constraints and merges the matrix decomposition process with cluster generation for optimized performance.
- EAMC: End-to-end Adversarial-attention network for Multi-modal Clustering (EAMC) [51] integrates adversarial learning with attention mechanisms to match the latent feature distributions across different modalities and assess the significance of each modality.
- SIMVC: Simple Multi-View Clustering (SiMVC) [31] uses a learnable linear combination to integrate representations from multiple views, which is both effective and intuitive.
- COMVC: Contrastive Multi-View Clustering (CoMVC) [31] builds upon SiMVC through the addition of a selective contrastive alignment module, maintaining view invariance while avoiding the pitfalls of representation alignment.
- SDSNE: Stationary Diffusion State Neural Estimation (SDSNE) [52] employs a fusion of multi-view structural information and a structure-level co-supervision learning strategy to achieve a static state in clustering tasks.
- MFLVC: Multi-level feature learning for contrastive multi-view clustering (MFLVC) [53] learns features at different levels from the original features and aligns them, thereby effectively achieving consistency goals across diverse feature spaces.
- GCFAGG: Global and Cross-view Feature Aggregation (GCFAgg) [54] aligns consensus representations and view-specific representations through a structure-oriented contrastive learning module.
- CSOT: learning Common Semantics via Optimal Transport (CSOT) [55] learns common semantics through optimal transmission and reweights samples according to their semantic importance.

Among the aforementioned methods, SMVSC, LMVSC, and OPMC are traditional MVC methods, while the rest are deep MVC methods.

In the experiments, we measure the performance of the models using four commonly employed evaluation metrics: clustering accuracy (ACC), normalized mutual information (NMI) [56], adjusted rand index (ARI) [57], and purity (PUR). Higher values for these metrics indicate better performance.

- ACC: It serves as one of the key evaluation metrics for measuring clustering performance, used to quantify the degree of correspondence between the clustering outcomes and the true labels. Given the predicted labels y and ground truth $y^{'}$, ACC is calculated as follows:

$$ACC = \frac{\sum_{i=1}^{N} \Psi\left(y_i, y_i^{'}\right)}{N}, \tag{14}$$

  where N represents the total number of samples, and $\Psi\left(y_i, y_i^{'}\right)$ is an indicator function that takes the value of 1 when $y_i = y_i^{'}$, and 0 otherwise.
- NMI: This metric assesses the similarity between the clustering results and the true labels. NMI is calculated as follows:

$$NMI\left(y, y^{'}\right) = \frac{2I\left(y, y^{'}\right)}{\left(H\left(y\right) + H\left(y^{'}\right)\right)}, \tag{15}$$

  where $I\left(.\right)$ denotes mutual information and $H\left(.\right)$ denotes cross-entropy.
- ARI: This metric is derived from an adjusted Rand Index (RI), with possible values spanning from -1 to 1. As its value gets closer to 1, it indicates that the clustering results are more realistic. ARI is calculated as follows:

$$ARI = \frac{RI - E\left[RI\right]}{\max\left(RI\right) - E\left(RI\right)}, \tag{16}$$

  where $E\left(RI\right)$ is the expected Rand Index.
- PUR: It computes the sum of samples in that class across all clusters and expresses this sum as a proportion of the total sample count. PUR is calculated using the following formula:

$$PUR = \sum_{i=1}^{C} \frac{K_i}{N} P_i, \tag{17}$$

  where K_i represents the count of samples within the i-th cluster from the clustering results, and P_i represents the proportion of samples that truly belong to the i-th cluster.

C. Implementation Details

For all datasets, the structure of each specific view encoder consists of a fully connected network. Specifically, the dimensions of each network are input-500-500-2000-512. The decoders have the opposite dimensional structure. In the experiments, we apply ReLU [58] as the activation function and opt for Adam [59] as the optimizer, setting the initial learning rate to 0.0001, the batch size to 256, and the temperature parameter τ to 0.5. For each view, the number of nearest neighbors is selected from the set $\{5, 7, 10\}$ to construct the nearest neighbor graph. The values of the two hyper-parameters λ_1 and λ_2 are chosen from the set $\{0.001, 0.01, 0.1, 1, 10, 100\}$.

The experimental environment consists of an Ubuntu Linux 22.04 platform outfitted with an NVIDIA 3090 GPU and

TABLE III: Clustering results on Wiki, Reuters, Hdigit, and ALOI datasets.

Datasets	LMVSC	SMVSC	OPMC	EAMC	SIMVC	COMVC	SDSNE	MFLVC	GCFAGG	CSOT	Ours
						ACC					
Wiki	17.96	16.39	19.33	50.48	55.09	53.45	56.32	41.38	57.22	48.22	**60.43**
Reuters	43.18	50.70	46.20	43.31	40.39	41.78	31.89	52.31	49.59	49.10	**59.07**
Hdigit	54.24	78.04	81.08	41.16	68.35	87.73	N/A	89.75	97.25	94.92	**99.54**
ALOI	50.34	35.21	53.54	15.08	71.43	75.43	N/A	59.00	76.31	65.46	**90.15**
Avg.	41.43	45.09	50.04	37.51	58.82	65.60	44.11	60.61	70.09	64.43	**77.14**
						NMI					
Wiki	4.21	10.80	6.21	49.89	52.10	51.51	52.86	38.47	48.77	43.98	**52.91**
Reuters	18.29	25.20	24.23	15.20	20.87	19.62	12.41	39.58	34.34	38.44	**39.87**
Hdigit	48.11	71.38	75.35	41.82	62.45	85.18	N/A	79.45	92.62	88.18	**98.58**
ALOI	70.65	64.61	74.24	50.68	89.75	90.92	N/A	85.62	89.51	82.78	**94.33**
Avg.	35.32	40.50	45.01	39.40	56.29	61.81	32.64	60.78	66.31	63.35	**71.42**
						ARI					
Wiki	2.16	34.26	2.73	37.05	41.30	40.61	38.92	26.60	37.94	32.83	**44.78**
Reuters	17.97	23.29	19.29	13.93	16.63	15.69	0.63	30.91	25.92	30.04	**32.34**
Hdigit	36.12	65.53	71.72	25.83	53.65	78.75	N/A	78.68	94.09	89.03	**98.98**
ALOI	36.95	17.84	40.00	5.86	69.50	71.31	N/A	54.75	71.71	57.52	**85.64**
Avg.	23.30	35.23	33.44	20.67	45.27	51.59	19.78	47.74	57.42	52.36	**65.44**

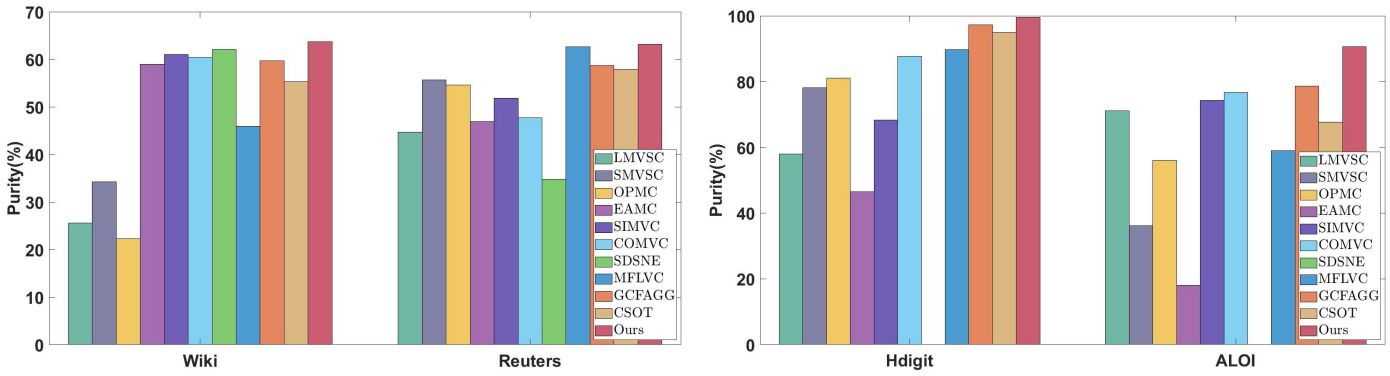

(a) PUR values on Wiki and Reuters datasets.

(b) PUR values on Hdigit and ALOI datasets.

Fig. 3: PUR values on four datasets.

32GB RAM. For the baseline methods used for comparison, we obtain the experimental results by following the recommended procedures using their publicly available code.

D. Experimental Results

Tables III, IV and Figs. 3, 4 demonstrate the experimental results of each baseline method on the five datasets. Bold text indicates the best results, the underlined text shows the second-best results, and 'N/A' indicates insufficient memory or time. From the data presented in these tables, we can specifically draw the following conclusions:

- Among the comparative methods, traditional MVC methods typically demonstrate lower performance relative to deep MVC methods. This disparity is attributed to the presence of redundant information within the original feature data, which often impedes traditional methods from effectively constructing graphs. In contrast, our approach demonstrates superior performance.
- Relative to other deep multi-view clustering methods, our approach demonstrates significant performance improvements. Specifically, in comparison to the second-best clustering results, our method attained ACC gains of 6.76%, 13.84%, and 9.08% on the Reuters, ALOI, and Caltech-5V datasets, respectively. This indicates that our method is capable of capturing information that is more conducive to clustering.
- These significant performance improvements can be attributed to our positive sample selection strategy guided by neighborhood consistency, which helps build more reliable positive sample pairs, mitigate the negative effects of false-negative pairs, and thus facilitate discriminative feature learning. Gaussian distribution modeling not only fully explores the embedded structural information of

TABLE IV: Clustering results on Caltech-XV datasets. "XV" denotes the number of views.

Datasets	LMVSC	SMVSC	OPMC	EAMC	SIMVC	COMVC	SDSNE	MFLVC	GCFAGG	CSOT	Ours
						ACC					
Caltech-2V	38.78	56.71	52.93	48.57	55.28	47.64	54.14	57.71	62.79	59.86	**65.79**
Caltech-3V	37.42	61.07	64.50	37.07	46.14	60.07	63.21	66.29	63.50	65.43	**75.50**
Caltech-4V	43.00	73.14	67.29	42.85	71.71	72.42	69.71	71.29	71.07	70.43	**84.86**
Caltech-5V	44.92	77.35	78.50	44.28	74.78	78.57	75.93	81.21	80.21	76.86	**90.29**
Avg.	41.03	67.07	65.81	43.19	61.98	64.68	65.75	69.13	69.39	68.15	**79.11**
						NMI					
Caltech-2V	28.82	43.50	35.73	43.14	48.33	41.16	45.66	53.26	49.04	52.11	**56.10**
Caltech-3V	25.50	49.92	49.42	25.90	40.28	56.42	55.40	58.12	53.19	57.75	**69.13**
Caltech-4V	34.49	61.91	57.81	29.15	66.29	66.36	65.56	68.45	61.14	65.57	**76.18**
Caltech-5V	31.67	71.51	67.00	33.07	66.91	72.15	74.29	70.53	68.90	65.56	**83.28**
Avg.	30.12	56.71	52.49	32.82	55.45	59.02	60.23	62.59	58.07	60.25	**71.17**
						ARI					
Caltech-2V	16.84	36.67	28.25	33.88	37.93	31.53	35.51	43.82	40.11	41.68	**45.59**
Caltech-3V	13.44	43.05	44.02	17.12	30.01	46.70	45.68	48.86	42.97	48.19	**60.25**
Caltech-4V	23.93	55.71	51.06	22.91	56.97	58.96	53.24	59.12	52.27	56.99	**70.02**
Caltech-5V	24.68	64.58	61.62	24.75	60.48	67.47	63.65	62.18	62.79	58.42	**81.21**
Avg.	19.72	50.00	46.24	24.67	46.35	51.17	49.52	53.50	49.54	51.32	**64.27**

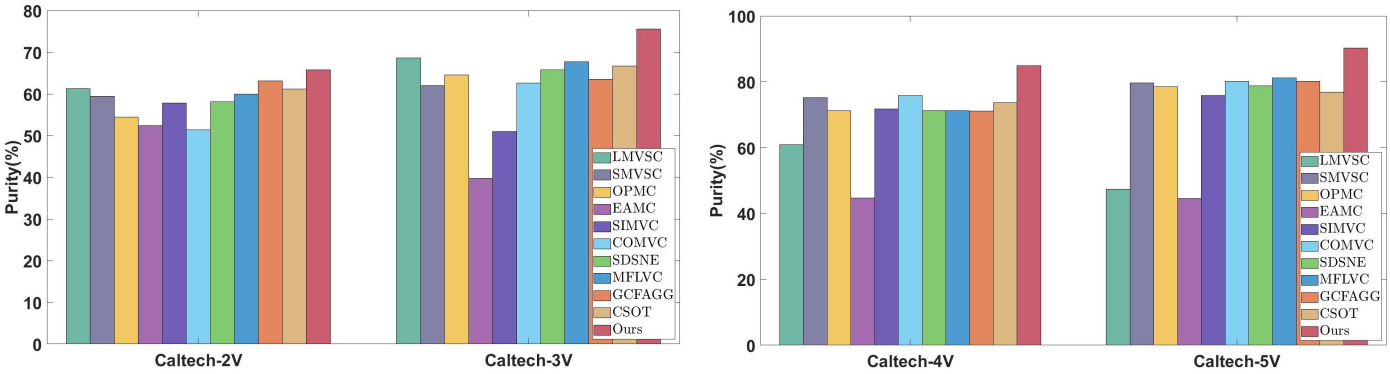

(a) PUR values on Caltech-2V and Caltech-3V datasets.

(b) PUR values on Caltech-4V and Caltech-5V datasets.

Fig. 4: PUR values on Caltech dataset.

views but also alleviates the representation differences between views, thereby improving the stability of samples within clusters.

E. Ablation Study

To evaluate the effectiveness of each component of our model, we perform ablation studies on the Wiki, Reuters, and ALOI datasets. The ablation results are presented in Table V.

- As detailed in Table V, the elimination of the local structure learning module resulted in ACC performance drops of 23.98% for the Reuters dataset and 25.96% for the ALOI dataset. The NMI performance also declined by 28.44% and 15.52%, respectively. This clearly demonstrates the importance of the neighborhood consistency-guided contrastive learning module, which significantly enhances the model's ability to learn discriminative features of samples, thereby greatly improving clustering performance.
- Similarly, we perform ablation studies on the embedding structure learning module. As can be observed from the results in the table, removing this module resulted in varying degrees of performance decline in both ACC and NMI across the three datasets. This demonstrates that the embedded structure learning module effectively addresses the differences in feature spaces between views by leveraging latent structural information, thereby enhancing clustering performance.

F. Visualization Analysis

To more effectively analyze our model's performance, we employ t-SNE [60] to visualize the feature representations learned during the training of the Caltech-5V dataset. From Fig. 5, it is evident that the clustering structures refine over time and become clearer as the training iterations increase. This visualization demonstrates the effectiveness of our model

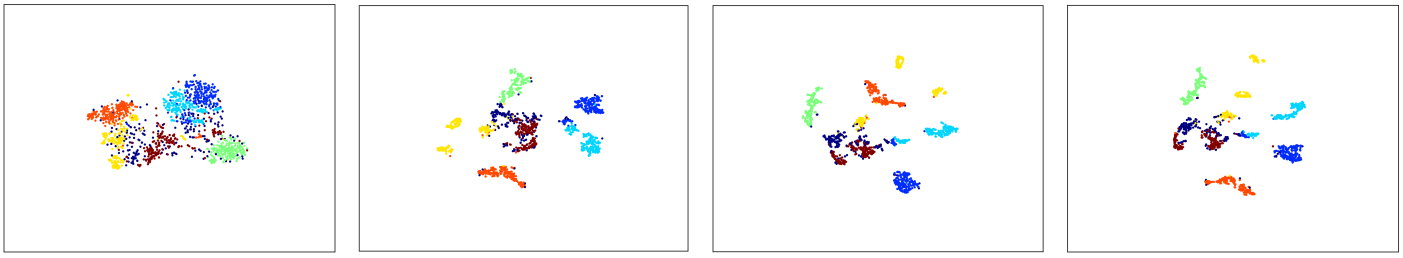

(a) Epoch 0 (b) Epoch 25 (c) Epoch 50 (d) Epoch 75

Fig. 5: Visualization of clustering results at different epochs on the Caltech-5V dataset.

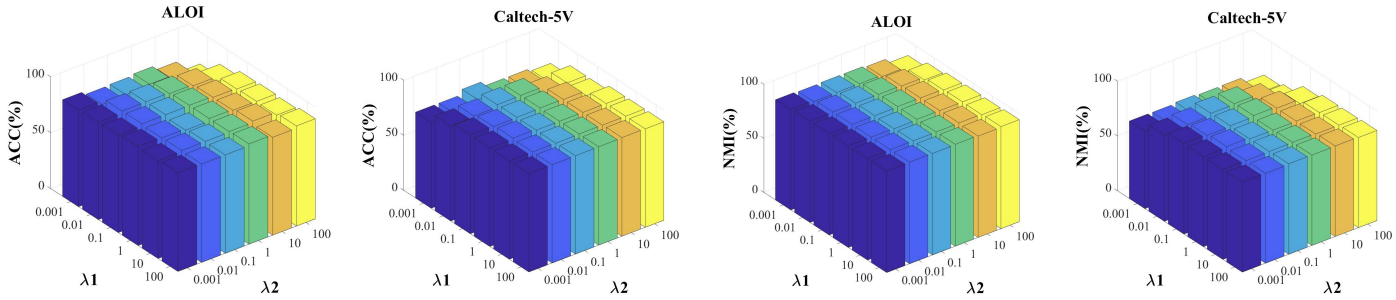

(a) (b) (c) (d)

Fig. 6: ACC and NMI performance of different λ_1 and λ_2 combinations on ALOI and Caltech-5V datasets.

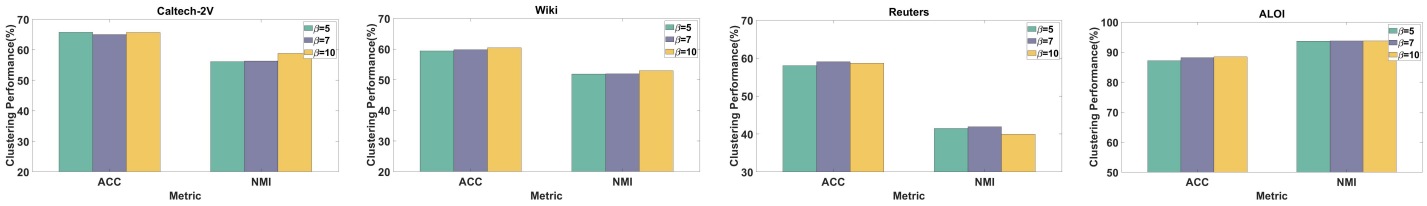

(a) (b) (c) (d)

Fig. 7: ACC and NMI performance with different k values on four datasets.

TABLE V: Ablation experiments on three datasets.

Datasets	Metrics	SGMVC	SGMVC (w/o $\mathcal{L}_{ls}$)	SGMVC (w/o $\mathcal{L}_{es}$)
Wiki	ACC	**60.43**	30.25	57.08
	NMI	**52.91**	21.44	50.63
	ARI	**44.78**	11.02	39.93
Reuters	ACC	**59.07**	35.09	55.44
	NMI	39.87	11.43	**43.31**
	ARI	**32.34**	11.78	30.81
ALOI	ACC	**90.15**	64.19	87.75
	NMI	**94.33**	78.81	94.32
	ARI	**85.64**	52.11	84.76

in integrating both local structural learning and embedding structural learning.

G. Parameter Analysis

We analyze the sensitivity of the hyper-parameters λ_1 and λ_2 in our method through experiments conducted on the ALOI and Caltech-5V datasets. In the experiments, the values of λ_1 and λ_2 are chosen from the set $\{0.001, 0.01, 0.1, 1, 10, 100\}$, and the experimental results for different parameter combinations are shown in Fig. 6. It is evident that the model typically exhibits stable performance concerning ACC and NMI, suggesting that our method is not sensitive to these hyper-parameters.

H. Convergence Analysis

Experiments were conducted on the Caltech-2V, Wiki, Reuters, and ALOI datasets to assess the proposed model's convergence and graph the corresponding loss and NMI curves. According to Fig. 9, the loss value experiences a quick reduction in the early stages of training and then slowly approaches a lower bound as more epochs are completed. These observations confirm that our model is flexible in selecting parameters.

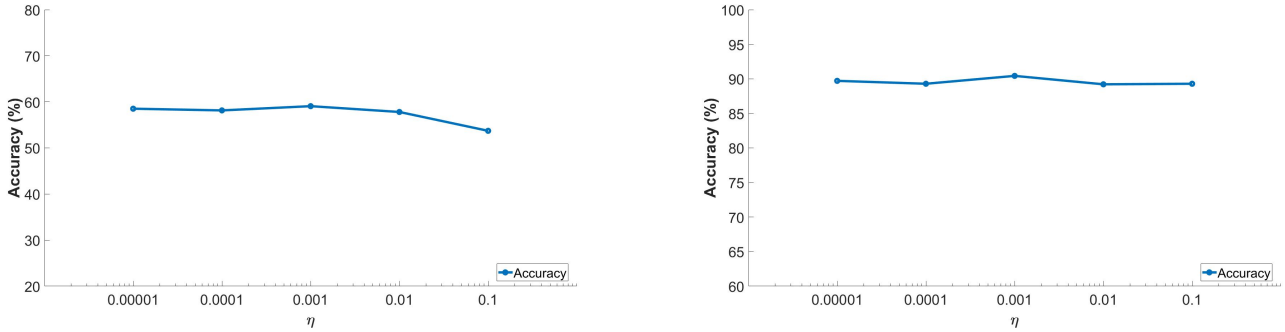

(a) Reuters Dataset (b) ALOI Dataset

Fig. 8: ACC performance with different η values on Reuters and ALOI datasets.

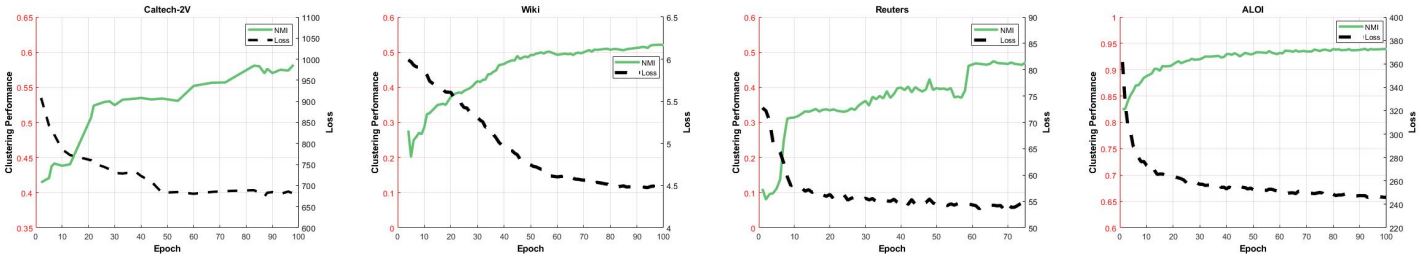

(a) Caltech-2v Dataset (b) Wiki Dataset (c) Reuters Dataset (d) ALOI Dataset

Fig. 9: The convergence analysis on Caltech-2v, Wiki, Reuters, and ALOI datasets.

V. CONCLUSION

In this paper, we propose a novel deep multi-view clustering method called SGMVC. Specifically, we introduce view-specific encoders for each view to capture view-specific information between views. We also design a cross-view consistent neighbor selection strategy to generate positive samples. In our method, an instance is considered as a true neighbor only if it is a mutual neighbor in both views. By introducing such intra-view structural information, the negative impact caused by false negatives can be reduced, which can facilitate the learning of consensus information and cross-view discriminative features. Additionally, we introduce a Gaussian distribution-based modeling strategy. By applying Gaussian modeling to the data of each view, our method uncovers latent structural information and optimizes feature embedding discrepancies for the same instance across different views, thus having the potential to achieve more consistent structural alignment. Extensive experiments validate that the effective combination of these two strategies significantly enhances clustering performance.

REFERENCES

[1] W. Kim, A. Kanezaki, and M. Tanaka, "Unsupervised learning of image segmentation based on differentiable feature clustering," *IEEE Transactions on Image Processing*, vol. 29, pp. 8055–8068, 2020.

[2] C. Wu and Z. Kang, "Robust entropy-based symmetric regularized picture fuzzy clustering for image segmentation," *Digital Signal Processing*, vol. 110, p. 102905, 2021.

[3] P. Hu, H. Zhu, J. Lin, D. Peng, Y.-P. Zhao, and X. Peng, "Unsupervised contrastive cross-modal hashing," *IEEE Transactions on Pattern Analysis and Machine Intelligence*, vol. 45, no. 3, pp. 3877–3889, 2022.

[4] J. Cui, Z. He, Q. Huang, Y. Fu, Y. Li, and J. Wen, "Structure-aware contrastive hashing for unsupervised cross-modal retrieval," *Neural Networks*, vol. 174, p. 106211, 2024.

[5] Y. Sun, Z. Ren, P. Hu, D. Peng, and X. Wang, "Hierarchical consensus hashing for cross-modal retrieval," *IEEE Transactions on Multimedia*, vol. 26, pp. 824–836, 2023.

[6] R. Agrawal, J. Gehrke, D. Gunopulos, and P. Raghavan, "Automatic subspace clustering of high dimensional data for data mining applications," in *Proceedings of the 1998 ACM SIGMOD international conference on Management of data*, 1998, pp. 94–105.

[7] K. A. Patel and P. Thakral, "The best clustering algorithms in data mining," in *2016 International Conference on Communication and Signal Processing (ICCSP)*. IEEE, 2016, pp. 2042–2046.

[8] C.-F. Tsai, H.-C. Wu, and C.-W. Tsai, "A new data clustering approach for data mining in large databases," in *Proceedings International Symposium on Parallel Architectures, Algorithms and Networks. I-SPAN'02*. IEEE, 2002, pp. 315–320.

[9] Z. Peng, H. Liu, Y. Jia, and J. Hou, "Egrc-net: Embedding-induced graph refinement clustering network," *IEEE Transactions on Image Processing*, vol. 32, pp. 6457–6468, 2023.

[10] Y. Qin, H. Wu, X. Zhang, and G. Feng, "Semi-supervised structured subspace learning for multi-view clustering," *IEEE Transactions on Image Processing*, vol. 31, pp. 1–14, 2021.

[11] S. Hu, Z. Shi, X. Yan, Z. Lou, and Y. Ye, "Multiview clustering with propagating information bottleneck," *IEEE Transactions on Neural Networks and Learning Systems*, 2023.

[12] X. Zhu, S. Zhang, W. He, R. Hu, C. Lei, and P. Zhu, "One-step multi-view spectral clustering," *IEEE Transactions on Knowledge and Data Engineering*, vol. 31, no. 10, pp. 2022–2034, 2018.

[13] L. Sun, J. Wen, C. Liu, L. Fei, and L. Li, "Balance guided incomplete multi-view spectral clustering," *Neural Networks*, vol. 166, pp. 260–272, 2023.

[14] S. Liu, X. Liu, S. Wang, X. Niu, and E. Zhu, "Fast incomplete multi-view clustering with view-independent anchors," *IEEE Transactions on Neural Networks and Learning Systems*, 2022.

[15] L. Li and H. He, "Bipartite graph based multi-view clustering," *IEEE transactions on knowledge and data engineering*, vol. 34, no. 7, pp. 3111–3125, 2020.

[16] S. Liu, S. Wang, P. Zhang, K. Xu, X. Liu, C. Zhang, and F. Gao, "Efficient one-pass multi-view subspace clustering with consensus anchors," in *Proceedings of the AAAI Conference on Artificial Intelligence*, vol. 36, no. 7, 2022, pp. 7576–7584.

[17] J. Wen, Z. Zhang, Y. Xu, and Z. Zhong, "Incomplete multi-view clustering via graph regularized matrix factorization," in *Proceedings of the European conference on computer vision (ECCV) workshops*, 2018, pp. 0–0.

[18] H. Zhao, Z. Ding, and Y. Fu, "Multi-view clustering via deep matrix factorization," in *Proceedings of the AAAI conference on artificial intelligence*, vol. 31, no. 1, 2017.

[19] X. Wan, J. Liu, X. Gan, X. Liu, S. Wang, Y. Wen, T. Wan, and E. Zhu, "One-step multi-view clustering with diverse representation," *IEEE Transactions on Neural Networks and Learning Systems*, 2024.

[20] X. Peng, J. Cheng, X. Tang, J. Liu, and J. Wu, "Dual contrastive learning network for graph clustering," *IEEE Transactions on Neural Networks and Learning Systems*, 2023.

[21] J. Jin, S. Wang, Z. Dong, X. Liu, and E. Zhu, "Deep incomplete multi-view clustering with cross-view partial sample and prototype alignment," in *Proceedings of the IEEE/CVF conference on computer vision and pattern recognition*, 2023, pp. 11 600–11 609.

[22] W. Lan, T. Yang, Q. Chen, S. Zhang, Y. Dong, H. Zhou, and Y. Pan, "Multiview subspace clustering via low-rank symmetric affinity graph," *IEEE Transactions on Neural Networks and Learning Systems*, 2023.

[23] J. Tang, Y. Lai, and X. Liu, "Multiview spectral clustering based on consensus neighbor strategy," *IEEE Transactions on Neural Networks and Learning Systems*, 2023.

[24] J. Cui, Y. Li, H. Huang, and J. Wen, "Dual contrast-driven deep multi-view clustering," *IEEE Transactions on Image Processing*, 2024.

[25] C. Cui, Y. Ren, J. Pu, J. Li, X. Pu, T. Wu, Y. Shi, and L. He, "A novel approach for effective multi-view clustering with information-theoretic perspective," *Advances in Neural Information Processing Systems*, vol. 36, 2024.

[26] H. Wang, Y. Yang, and B. Liu, "Gmc: Graph-based multi-view clustering," *IEEE Transactions on Knowledge and Data Engineering*, vol. 32, no. 6, pp. 1116–1129, 2019.

[27] Z. Lin, Z. Kang, L. Zhang, and L. Tian, "Multi-view attributed graph clustering," *IEEE Transactions on knowledge and data engineering*, vol. 35, no. 2, pp. 1872–1880, 2021.

[28] J. Wang, C. Tang, Z. Wan, W. Zhang, K. Sun, and A. Y. Zomaya, "Efficient and effective one-step multiview clustering," *IEEE Transactions on Neural Networks and Learning Systems*, 2023.

[29] S. Luo, C. Zhang, W. Zhang, and X. Cao, "Consistent and specific multi-view subspace clustering," in *Proceedings of the AAAI conference on artificial intelligence*, vol. 32, no. 1, 2018.

[30] Y. Wang, X. Lin, L. Wu, W. Zhang, Q. Zhang, and X. Huang, "Robust subspace clustering for multi-view data by exploiting correlation consensus," *IEEE Transactions on Image Processing*, vol. 24, no. 11, pp. 3939–3949, 2015.

[31] D. J. Trosten, S. Lokse, R. Jenssen, and M. Kampffmeyer, "Reconsidering representation alignment for multi-view clustering," in *Proceedings of the IEEE/CVF conference on computer vision and pattern recognition*, 2021, pp. 1255–1265.

[32] H. Tang and Y. Liu, "Deep safe multi-view clustering: Reducing the risk of clustering performance degradation caused by view increase," in *Proceedings of the IEEE/CVF Conference on Computer Vision and Pattern Recognition*, 2022, pp. 202–211.

[33] J. Cheng, Q. Wang, Z. Tao, D. Xie, and Q. Gao, "Multi-view attribute graph convolution networks for clustering," in *Proceedings of the twenty-ninth international conference on international joint conferences on artificial intelligence*, 2021, pp. 2973–2979.

[34] W. Xia, S. Wang, M. Yang, Q. Gao, J. Han, and X. Gao, "Multi-view graph embedding clustering network: Joint self-supervision and block diagonal representation," *Neural Networks*, vol. 145, pp. 1–9, 2022.

[35] Y. Zhang, F. Tian, C. Ma, M. Li, H. Yang, Z. Liu, E. Zhu, and X. Liu, "Regularized instance weighting multiview clustering via late fusion alignment," *IEEE Transactions on Neural Networks and Learning Systems*, 2024.

[36] K. He, H. Fan, Y. Wu, S. Xie, and R. Girshick, "Momentum contrast for unsupervised visual representation learning," in *Proceedings of the IEEE/CVF conference on computer vision and pattern recognition*, 2020, pp. 9729–9738.

[37] T. Chen, S. Kornblith, M. Norouzi, and G. Hinton, "A simple framework for contrastive learning of visual representations," in *International conference on machine learning*. PMLR, 2020, pp. 1597–1607.

[38] G. Zou, Y. Ye, T. Chen, and S. Hu, "Learning dual enhanced representation for contrastive multi-view clustering," in *Proceedings of the 32nd ACM International Conference on Multimedia*, 2024, pp. 8731–8739.

[39] W. Xia, T. Wang, Q. Gao, M. Yang, and X. Gao, "Graph embedding contrastive multi-modal representation learning for clustering," *IEEE Transactions on Image Processing*, vol. 32, pp. 1170–1183, 2023.

[40] Z. Wang, Y. Du, Y. Wang, R. Ning, and L. Li, "Deep incomplete multi-view clustering via multi-level imputation and contrastive alignment," *Neural Networks*, vol. 181, p. 106851, 2025.

[41] Z. Huang, J. Chen, J. Zhang, and H. Shan, "Learning representation for clustering via prototype scattering and positive sampling," *IEEE Transactions on Pattern Analysis and Machine Intelligence*, vol. 45, no. 6, pp. 7509–7524, 2022.

[42] X. Chen and K. He, "Exploring simple siamese representation learning," in *Proceedings of the IEEE/CVF conference on computer vision and pattern recognition*, 2021, pp. 15 750–15 758.

[43] L. Fei-Fei, R. Fergus, and P. Perona, "Learning generative visual models from few training examples: An incremental bayesian approach tested on 101 object categories," in *2004 conference on computer vision and pattern recognition workshop*. IEEE, 2004, pp. 178–178.

[44] Y. Sun, Y. Qin, Y. Li, D. Peng, X. Peng, and P. Hu, "Robust multi-view clustering with noisy correspondence," *IEEE Transactions on Knowledge and Data Engineering*, 2024.

[45] C. Apté, F. Damerau, and S. M. Weiss, "Automated learning of decision rules for text categorization," *ACM Transactions on Information Systems (TOIS)*, vol. 12, no. 3, pp. 233–251, 1994.

[46] M.-S. Chen, J.-Q. Lin, X.-L. Li, B.-Y. Liu, C.-D. Wang, D. Huang, and J.-H. Lai, "Representation learning in multi-view clustering: A literature review," *Data Science and Engineering*, vol. 7, no. 3, pp. 225–241, 2022.

[47] G.-Y. Zhang, D. Huang, and C.-D. Wang, "Facilitated low-rank multi-view subspace clustering," *Knowledge-Based Systems*, vol. 260, p. 110141, 2023.

[48] Z. Kang, W. Zhou, Z. Zhao, J. Shao, M. Han, and Z. Xu, "Large-scale multi-view subspace clustering in linear time," in *Proceedings of the AAAI conference on artificial intelligence*, vol. 34, no. 04, 2020, pp. 4412–4419.

[49] M. Sun, P. Zhang, S. Wang, S. Zhou, W. Tu, X. Liu, E. Zhu, and C. Wang, "Scalable multi-view subspace clustering with unified anchors," in *Proceedings of the 29th ACM international conference on multimedia*, 2021, pp. 3528–3536.

[50] J. Liu, X. Liu, Y. Yang, L. Liu, S. Wang, W. Liang, and J. Shi, "One-pass multi-view clustering for large-scale data," in *Proceedings of the IEEE/CVF international conference on computer vision*, 2021, pp. 12 344–12 353.

[51] R. Zhou and Y.-D. Shen, "End-to-end adversarial-attention network for multi-modal clustering," in *Proceedings of the IEEE/CVF conference on computer vision and pattern recognition*, 2020, pp. 14 619–14 628.

[52] C. Liu, Z. Liao, Y. Ma, and K. Zhan, "Stationary diffusion state neural estimation for multiview clustering," in *Proceedings of the AAAI Conference on Artificial Intelligence*, vol. 36, no. 7, 2022, pp. 7542–7549.

[53] J. Xu, H. Tang, Y. Ren, L. Peng, X. Zhu, and L. He, "Multi-level feature learning for contrastive multi-view clustering," in *Proceedings of the IEEE/CVF conference on computer vision and pattern recognition*, 2022, pp. 16 051–16 060.

[54] W. Yan, Y. Zhang, C. Lv, C. Tang, G. Yue, L. Liao, and W. Lin, "Gcfagg: Global and cross-view feature aggregation for multi-view clustering," in *Proceedings of the IEEE/CVF Conference on Computer Vision and Pattern Recognition*, 2023, pp. 19 863–19 872.

[55] Q. Zhang, L. Zhang, R. Song, R. Cong, Y. Liu, and W. Zhang, "Learning common semantics via optimal transport for contrastive multi-view clustering," *IEEE Transactions on Image Processing*, 2024.

[56] S. Hu, G. Zou, C. Zhang, Z. Lou, R. Geng, and Y. Ye, "Joint contrastive triple-learning for deep multi-view clustering," *Information Processing & Management*, vol. 60, no. 3, p. 103284, 2023.

[57] L. Hubert and P. Arabie, "Comparing partitions," *Journal of classification*, vol. 2, pp. 193–218, 1985.

[58] X. Glorot, A. Bordes, and Y. Bengio, "Deep sparse rectifier neural networks," in *Proceedings of the fourteenth international conference on artificial intelligence and statistics*. JMLR Workshop and Conference Proceedings, 2011, pp. 315–323.

[59] D. P. Kingma, "Adam: A method for stochastic optimization," *arXiv preprint arXiv:1412.6980*, 2014.

[60] L. Van der Maaten and G. Hinton, "Visualizing data using t-sne." *Journal of machine learning research*, vol. 9, no. 11, 2008.

Jinrong Cui received the Ph.D. degree in computer science and technology from the Harbin Institute of Technology, Shenzhen, China, in 2015. She is currently as an Assistant Professor with the College of Mathematics and Informatics, South China Agricultural University, Guangzhou, China. Her current research interests include image and video enhancement, pattern recognition and machine learning.

Xiaohuang Wu is currently pursuing the master's degree with the College of Mathematics and Informatics, South China Agricultural University, Guangzhou, China. His current research interests include machine learning and unsupervised learning.

Haitao Zhang is an associate professor at the University of Electronic Science and Technology of China and graduated from Tsinghua University. He has published more than ten papers in top journals and conferences and holds more than ten invention patents. His research areas include drones, eVTOL, intelligent unmanned systems, artificial intelligence control, etc. He has won numerous awards and honors, including Tsinghua University Outstanding Undergraduate, Liangjiang Outstanding Postdoctoral Fellow, Shenzhen Pengcheng Peacock Plan High-level Talent, etc. He is a reviewer for many famous journals and conferences.

Chongjie Dong is an associate professor with a master's degree. His primary research areas focus on network software development and the application of artificial intelligence technology. In recent years, he has published over 20 educational and research papers, including 4 Chinese core journal articles. Additionally, he has presided over 5 provincial and municipal projects.

Jie Wen (Senior Member, IEEE) received the Ph.D. degree in Computer Science and Technology at Harbin Institute of Technology, Shenzhen in 2019. He is currently an Associate Professor at the School of Computer Science and Technology, Harbin Institute of Technology, Shenzhen. His research interests include image and video enhancement, pattern recognition, and machine learning. He has authored or co-authored more than 100 technical papers at prestigious international journals and conferences, including the TNNLS, TIP, TCYB, NeurIPS, ICML, CVPR, AAAI, IJCAI, ACM MM, etc. He serves as an **Associate Editor** of *IEEE Transactions on Image Processing*, *IEEE Transactions on Information Forensics and Security*, *Pattern Recognition*, and *International Journal of Image and Graphics*, an **Area Editor** of *Information Fusion*. He also served as the **Area Chair** of *ACM MM* and *ICML*. He was selected for the 'World's Top 2% Scientists List' in 2021-2024. One paper received the 'distinguished paper award' from AAAI'23. For more information, please refer to the homepage: https://sites.google.com/view/jerry-wen-hit/home.